Study of Seismic Hazard and Risk Using Classical Probabilistic Seismic Hazard Analysis (PSHA) in the Rif Chain using Openquake Engine

Ismail Bouabid, Kamal Agharroud, Souad El Bakali Ettahiri, Hanane Reddad

Geosciences Laboratory, Faculty of Sciences Ain Chok, Hassan II University, Casablanca, Morocco

Abstract

This study presents a probabilistic seismic hazard assessment (PSHA) for the Rif region in northern Morocco, using the OpenQuake Engine to incorporate both fault-based and distributed seismic sources within a unified modeling framework. Active faults were modeled using moment-balanced truncated Gutenberg–Richter distributions, while background seismicity was represented through nine distributed zones derived from local catalogs and characterized by incremental magnitude-frequency distributions (MFDs). A logic tree was used to combine source models and ground motion prediction equations (GMPEs) relevant to active shallow crustal regions.

Hazard calculations were performed for peak ground acceleration (PGA) at exceedance probabilities of 50%, 10%, 5%, and 2% in 50 years. The results show that several cities, including Al Hoceima, Fès, and Meknès, are subject to significantly higher ground shaking than prescribed by the Moroccan seismic design code (RPS v2011). Mean PGA values at 10% exceedance exceed 0.35 g in these areas, compared to the 0.14–0.18 g ranges specified in the code. These discrepancies suggest that the current national zonation underestimates seismic hazard in several tectonically active regions.

The model developed in this study is intended to shed light on the need to revise and enhance Morocco's seismic hazard framework. By integrating detailed fault geometries, updated seismicity data, and regionally calibrated ground motion prediction models, the study provides a scientifically grounded perspective that can guide and support future improvements to national seismic zonation. These insights contribute to more accurate seismic risk assessment and the development of resilient, risk-informed design standards.

Keywords: Probabilistic Seismic Hazard Analysis, Peak Ground Acceleration (PGA), Earthquakes, Rif chain, OpenQuake Engine

1. Introduction

The Rif chain located in northern Morocco lies at the convergence zone between the African and Eurasian tectonic plates and is widely recognized as one of the most seismically active areas in the western Mediterranean (Agharroud et al., 2021). Tectonic deformation in this region is accommodated through a complex interplay of thrust, strike-slip, and normal faulting, reflecting a mixed compressional and extensional regime (Poujol et al., 2014; Akka et al., 2022). This geodynamic context has produced numerous moderate to strong earthquakes in the instrumental period, including the Mw 6.0 Al Hoceima earthquake in 1994 and the Mw 6.3 Al Hoceima earthquake in 2004, which caused significant damage and loss of life (El Alami and Tadili, 2002; Stich et al., 2006).

Despite its seismic relevance, Probabilistic Seismic Hazard Assessment (PSHA) in the Rif chain remains limited and often rely on simplified source models that fail to integrate both fault-specific and distributed seismicity. existing studies treat seismicity as spatially smoothed zones or rely exclusively on historical catalogs, potentially overlooking the contribution of mapped active fault structures and their associated rupture characteristics (Poggi et al., 2020).

The present study aims to address these limitations by applying a classical Probabilistic Seismic Hazard Analysis (PSHA) approach using the OpenQuake Engine, which allows for detailed source modelling, site-specific ground motion calculation, and rigorous uncertainty treatment via logic trees. Our model incorporates nine known active faults segments in the Rif, each characterized by geometry, slip rate, magnitude-frequency distribution (MFD), and probabilistic distributions of strike, dip, rake, and hypocentral depth. In parallel, we construct a distributed seismicity model derived from the declustered USGS catalog (1950–2025) to capture background seismicity.

To better reflect local site amplification effects, spatially variable VS30 (shear-wave velocity for the top 30 meters) measurements derived from the United States Geological Survey (USGS) database were integrated at over 1500 locations. Ground motion was modeled using a weighted logic tree of three GMPEs selected for active shallow crustal regions. The outputs include hazard maps, hazard curves, and peak ground acceleration (PGA) estimates at various probabilities of exceedance over a 50-year period.

2. Geological and Seismotectonic Setting

The Rif chain, located in northern Morocco, represents the southern margin of the complex convergent boundary between the African and Eurasian plates (Pedrera et al., 2011). It forms the southern part of the arcuate Gibraltar Arc system and is geologically continuous with the Betic Cordillera in southern Spain. This zone accommodates an active and distributed deformation field resulting from oblique plate convergence at a rate of approximately 3–5 mm/year (DeMets et al., 2010).

Tectonic deformation in the Rif is characterized by crustal shortening, uplift, and distributed strike-slip motion accommodated along multiple fault systems that exhibit reverse, strike-slip, and normal faulting mechanisms (Poujol et al., 2014; Akka et al., 2022). The region has been shaped by complex geodynamic processes, including slab rollback and lithospheric delamination (Lonergan and White, 1997), although the recent tectonic evolution and driving mechanisms remain debated.

The current tectonic development of the Rif chain is primarily driven by the ongoing compression in the Moroccan Rif and the formation of the active Trans-Alboran shear zone (Fig. 1). This has led to the formation of multiple active faults across the Rif region, such as the Nekor fault, which function as lateral ramps

for major thrust fronts (Morel, 1994). Additionally, the Al Hoceima fault system (comprising the Ajdir, Imzouren, and Boujibar segments (e.g., Lafosse et al., 2016)) as well as the Boudinar and Trougout faults (Poujol et al., 2014), have been activated. Furthermore, a series of thrust systems in the southern Rif, including the Zerhoun, Zbidate, Kennoufa, El Merga, and Tratt faults, have also reactivated (Agharroud et al., 2021).

Seismological records and focal mechanism studies confirm the coexistence of compressional and extensional tectonic regimes in the Rif, with major earthquakes aligning closely with mapped surface or subsurface faults. Notable examples include the Mw 6.0 Imzouren earthquake in 1994 and the Mw 6.4 Al Hoceima earthquake in 2004. The 2004 event, in particular, exhibited predominant strike-slip motion with a minor normal component, reflecting strain partitioning along two fault branches, one mainly strike-slip and the other more extensional (Van der Woerd et al., 2014).

In addition to the well-mapped fault structures, the Rif chain exhibits a widespread distribution of microseismicity (Fig:1), This seismicity is not restricted to major fault traces but is instead dispersed across region, particularly in the central and eastern Rif, as revealed by instrumental earthquake catalogs. These smaller-magnitude events are not always directly associated with recognized fault traces, suggesting the presence of blind or unmapped faults, as well as diffuse strain accommodation across the crust.

This pattern of distributed seismicity reflects the complex deformation regime of the area and highlights the

limitations of fault-only models. Therefore, to achieve a comprehensive representation of seismic sources in the region, it is essential to incorporate both fault-based sources and a distributed background seismicity model, ensuring that both localized and diffuse seismic hazards are adequately captured

3. Methodology

3.1 Overview

This study applies a classical probabilistic seismic hazard analysis (PSHA) using the OpenQuake Engine v3.23. The model integrates fault-based seismic sources with a distributed background seismicity component and incorporates ground motion prediction and site condition data via logic trees. Hazard values were computed for peak ground acceleration (PGA) at multiple exceedance probabilities over a 50-year exposure period.

3.2 Seismic Source Characterization

3.2.1 Fault-Based Sources

The fault-based model includes nine active faults identified from geological and seismotectonic studies within the Rif region. These faults were implemented as (simple Fault Source) objects, each defined by its surface trace, dip angle, and seismogenic depth extent. In the absence of detailed data, a uniform dip angle of 50° and seismogenic depth range of 0–20 km was assumed for all faults.

The geometry of each fault was digitized as a polyline using surface fault traces available in geological literature and maps. Fault lengths were computed from these traces, and fault widths were calculated as a function of depth and dip. A tectonic region type of Active Shallow Crust was assigned uniformly.

Slip rates for each fault were derived from published literature based on local and regional tectonics. These values ranged from 0.15 mm/yr to 2.3 mm/yr. The seismic moment rate for each fault was computed using the equation:

$$M_0=\mu \cdot A \cdot D \quad (1)$$

where M_0 = Seismic moment
$\mu = 3\times10^{10}$ Pa is the shear modulus
A = Fault rupture area (m^2)
D = is the slip rate in m/yr

For each fault, a Truncated Gutenberg-Richter (TGR) magnitude-frequency distribution was assigned to characterize expected seismicity. A uniform b-value of 1.0 was assumed for all faults, consistent with regional tectonic settings and global crustal averages. The minimum magnitude was fixed at 5.0 for all fault sources to reflect the lower threshold of potentially damaging earthquakes.
The maximum magnitude (M_{max})was estimated based on fault trace length using the empirical relationship from Wells and Coppersmith (1994), which links rupture length to expected earthquake magnitude was used:

$$M_{max}=5.08+1.16\log_{10}(L) \quad (2)$$

Where (L) is the fault length in kilometers.

The a-value of each fault's magnitude-frequency distribution was not arbitrarily chosen. Instead, it was determined using a moment-rate balancing approach, which ensures that the amount of seismic energy released over time matches the energy expected from tectonic loading.
it was calculated such that the total seismic moment released per year by the MFD, across all magnitudes from M_{min} to M_{max} matches the tectonic moment rate. This condition is expressed by the equation:

$$\dot{M}_0 = \int_{M_{min}}^{M_{max}} 10^{a-bM} \cdot 10^{1.5M+9.1}\, dM \quad (3)$$

where:
M_0: is the tectonic moment rate (Nm/year)
10^{a-bM}: is the annual rate of earthquakes at magnitude M
$10^{1.5M+9.1}$: is the seismic moment of an earthquake at magnitude *M* (Hanks & Kanamori, 1979)

This integral was solved numerically for each fault by adjusting a-value until the total modeled seismic moment release matched the fault's tectonic moment rate. This ensures that each fault's recurrence model is both physically realistic and consistent with its long-term slip behaviour.

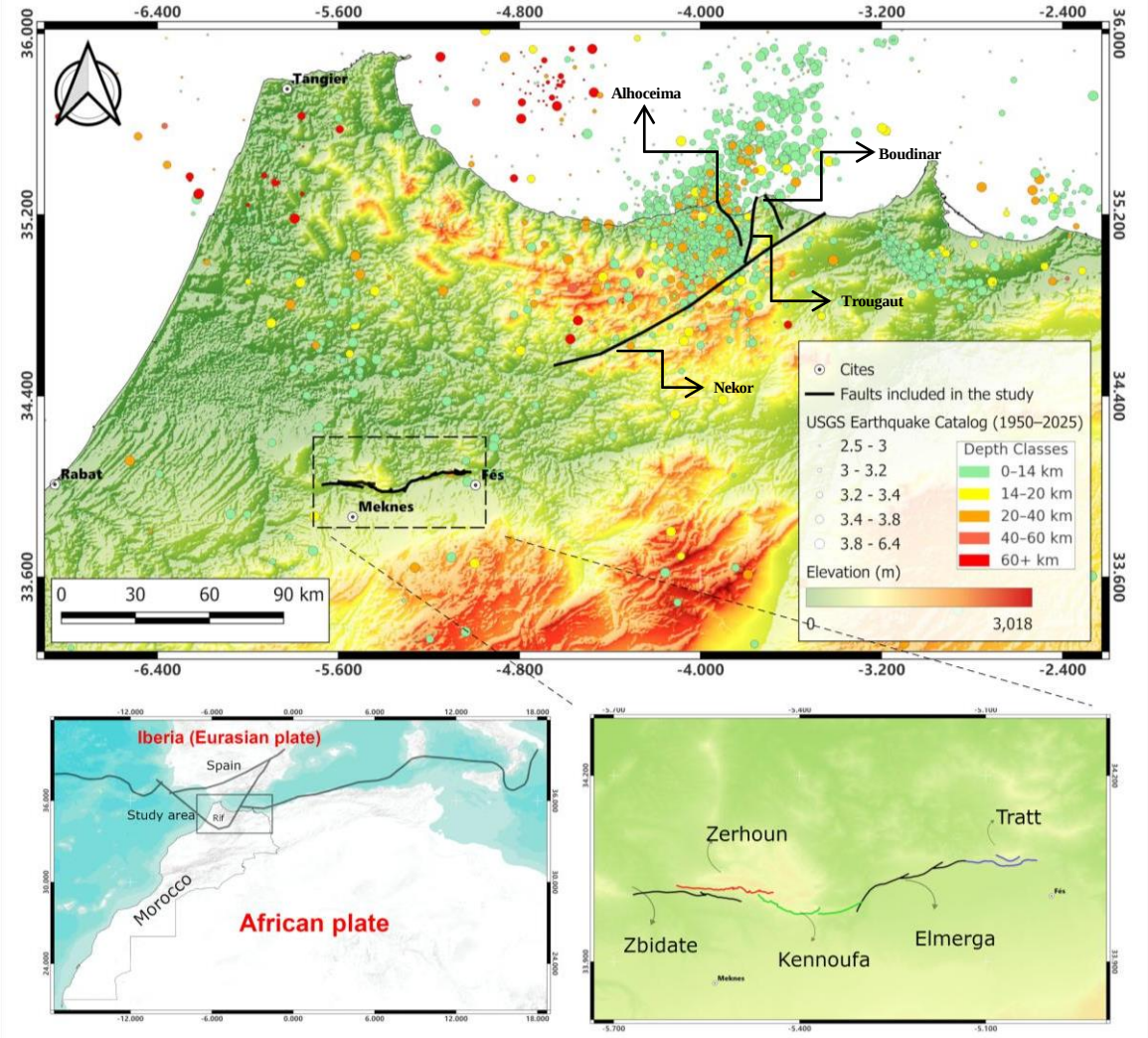

Figure 1: Study area overview showing fault traces and distributed seismicity zone boundaries across the Rif region

Table 1: Summary of fault source parameters used in the PSHA model. The parameters include slip rate, maximum magnitude (Mmax), and probabilistic definitions of fault geometry (strike, dip, rake) and hypocentral depth.

Fault Name	Slip Rate (mm/yr)	Mmin	Mmax	b-value	a-value (computed)	Nodal Plane Dist. (strike/dip/rake)	Hypocentral Depth Dist.
Nekor Fault	2.3	5	6.2	1	4.54	65/60/-90 (P=0.6) 60/75/-90 (P=0.4)	10.0 km (P=0.6); 12.0 km (P=0.4)
Boudinar Fault	0.6	5	5.9	1	3.96	60/75/-90 (P=0.5) 60/70/-90 (P=0.5)	7.0 km (P=0.5); 9.0 km (P=0.5)
Al Hoceima Fault	1.2	5	6	1	4.33	50/80/-90 (P=0.7) 50/75/-100 (P=0.3)	8.0 km (P=0.5); 12.0 km (P=0.2)
Trougout Fault	0.15	5	5.6	1	3.29	70/80/-90 (P=0.5) 70/75/-90 (P=0.5)	8.0 km (P=0.5) 10.0 km (P=0.5)
Zerhoun Fault	0.5	5	5.8	1	3.81	100/45/90 (P=0.6) 105/40/90 (P=0.4)	6.0 km (P=0.6) 0.0 km (P=0.4)

Zbidate Fault	0.6	5	5.7	1	3.73	100/45/90 (P=0.6) 105/40/90 (P=0.4)	6.0 km (P=0.6) 14.0 km (P=0.4)
Kennoufa Fault	0.6	5	5.9	1	3.99	100/45/90 (P=0.6) 105/40/90 (P=0.4)	6.0 km (P=0.6) 10.0 km (P=0.4)
El Merga Fault	0.3	5	5.5	1	3.19	110/60/-170 (P=0.5) 115/55/-170 (P=0.5)	7.0 km (P=0.5) 9.0 km (P=0.5)
Tratt Fault	0.9	5	5.8	1	3.98	95/45/90 (P=0.6) 100/40/90 (P=0.4)	6.0 km (P=0.5) 9.0 km (P=0.5)

Uncertainties in fault parameters such as dip, rake, strike, and hypocenter depth were handled inside the fault definitions themselves. Instead of using separate logic tree branches for these features, probabilistic distributions were assigned directly to the faults. This method allows a more realistic and detailed
representation of how faults behave in the

3.2.2 Distributed Seismicity Source

To complement the fault-based model, a distributed seismicity framework was implemented to capture background seismicity not explicitly assigned to known active faults. The study region was subdivided into nine area source zones, based on the seismotectonic classification proposed by Pelaez et al (see figure 2 below), which accounts for geological and geophysical characteristics across the Rif region.

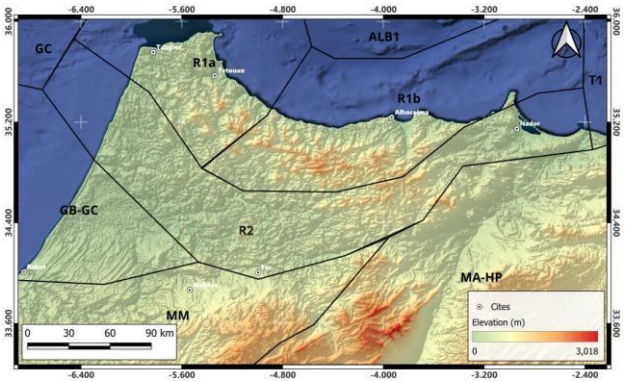

Figure 2: Seismotectonic zoning of the Rif region adapted from Pelaez et al. (2007), showing the division into distinct distributed seismicity zones based on geological and seismic criteria

For each zone, a separate seismic catalog was extracted from a homogenized, declustered regional catalog spanning the period 1950–2025. These zone-specific catalogs were processed to compute incremental magnitude-frequency distributions (MFDs) using a constant bin width of 0.1 magnitude units.
Incremental MFDs were preferred over truncated Gutenberg-Richter distributions because they are empirically driven and directly reflect observed seismicity. This choice helps avoid the potential overestimation of hazard in zones with sparse or incomplete catalogs, where fitting a parametric GR distribution could extrapolate large-magnitude rates beyond what the data supports.

All nine distributed sources were defined as areaSource objects with a tectonic region type of Active Shallow Crust, A uniform seismogenic depth range of 0–20 km was assigned. Default nodal plane and hypocentral depth distributions were applied uniformly across all zones,
The seismic catalog was homogenized by converting all magnitudes to moment magnitude (Mw). For local and duration magnitudes (ML, Md), the empirical relation $Mw = 0.85 \times M + 0.27$ was applied, following Johnston (1996) and Hanks and Kanamori (1979). Body-wave and regional magnitudes (Mb, MbLg) were converted using $Mw = 0.85 \times M + 1.03$, consistent with regional studies (e.g., Atkinson and Boore, 1995). Surface-wave magnitudes (Ms) were transformed using the global relation $Mw = 0.67 \times Ms + 2.07$ proposed by Scordilis (2006). Events originally reported in moment magnitude scales (Mw, Mww, Mwb, Mwr, Mwc) were retained without modification. This homogenization enables consistent magnitude–frequency analysis and reliable seismic hazard assessment.
The catalog was then declustered using the Gardner and Knopoff (1974) algorithm to remove dependent events and retain only mainshocks, ensuring compliance with the Poissonian assumption required for probabilistic seismic hazard modeling.

3.2.3 Ground Motion Modeling

Ground motion was estimated using a logic tree combining three ground motion prediction equations (GMPEs), each calibrated for shallow crustal tectonic environments:

- Akkar et al. (2014) – weight: 0.4
- Boore et al. (2014) – weight: 0.3
- Bindi et al. (2014) – weight: 0.3

These GMPEs were specifically chosen for their calibration to active shallow crustal tectonic environments, consistent with the seismotectonic characteristics of the Rif region. Akkar et al. (2014) and Bindi et al. (2014) are based on extensive European and Mediterranean datasets, offering regionally tailored predictions, while Boore et al. (2014) provides a globally robust model for active shallow crustal seismicity. The assigned weights reflected both the regional relevance of each model and their demonstrated performance in similar tectonic contexts, ensuring a balanced representation of ground motion variability for the study area.

3.2.4 Site Model

Site amplification effects were modeled using VS30 values from the United States Geological Survey (USGS) global dataset, which estimates the shear-wave velocity in the upper 30 meters of the subsurface. Although this dataset includes over 1,500 points across the study area, it is based on global topographic and geological proxies rather than direct measurements. These values were incorporated into the OpenQuake site model (site_model.csv) to account for first-order site effects in the hazard calculations.

However, the lack of locally measured geophysical data introduces uncertainty, and the results should be interpreted with caution in terms of local site amplification.

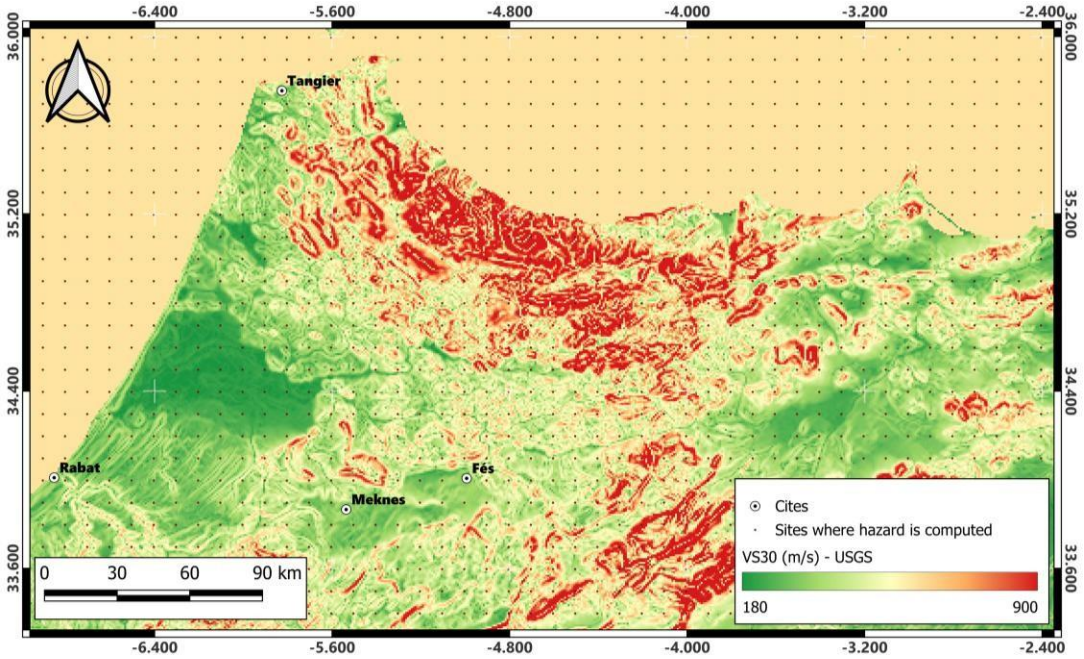

Figure 3: Spatial distribution of VS30 values (shear-wave velocity in the upper 30 meters) used for site-specific hazard calculation. Values are derived from the USGS database and interpolated across more than 1,500 locations in the Rif region.
These values are estimated from global topographic and geological proxies and do not reflect direct in situ geophysical measurements. While might be useful for regional-scale analysis, they introduce uncertainties in local site response estimation

3.2.5 Logic Tree Configuration

In this study, a single-branch logic tree was used for the seismic source model. This branch combines both the fault-based sources and the distributed seismicity sources in one model. The reason for this approach is that while major faults are known and well-mapped in the Rif region, a significant portion of seismicity cannot be directly linked to mapped faults. Therefore, the distributed seismicity model is used to account for this background seismicity, including smaller, scattered earthquakes and events originating on unmapped or poorly understood faults.

By including both source types within the same logic tree branch, the model reflects the understanding that both known faults and diffuse seismicity contribute to the regional hazard. The fault sources account for larger, well-constrained ruptures, while the area sources represent more dispersed seismicity not captured by the fault model.

The fault-based sources and distributed seismicity sources were defined separately and then combined within a single logic tree branch. This branch was assigned a weight of 1.0, meaning it represents the only configuration used in the seismic hazard calculations. By combining both source types in a single branch, where known faults are responsible for the most significant earthquakes, and distributed sources capture background activity and seismicity from less well-defined structures.

3.2.5.1 GMPE Logic Tree

To estimate how ground shaking decreases with distance and varies with earthquake magnitude, a logic tree of ground motion prediction equations (GMPEs) was used. These equations are an essential part of the seismic hazard model, and help predict how strong the shaking will be at a site, given an earthquake of a certain size and distance.

Three GMPEs were selected because they are all developed for active shallow crust regions — the same tectonic setting as in the Rif area. The selected models are:

- Akkar et al. (2014) — weight: 0.4
- Boore et al. (2014) — weight: 0.3
- Bindi et al. (2014) — weight: 0.3

These GMPEs were chosen based on their applicability to the region and their widespread use in similar studies. Akkar et al. (2014) was given the highest weight because it includes strong-motion data from Europe and the Mediterranean, making it particularly relevant. Boore et al. (2014) is commonly used in international hazard assessments and is known for its reliability in active crustal settings. Bindi et al. (2014) is also well suited to the Euro-Mediterranean context and complements the other two models.

Due to the absence of strong-motion recordings specific to Morocco, it was not possible to perform a detailed calibration or statistical evaluation of the selected GMPEs.
As a result, all three models were retained in the logic tree with equal or nearly equal weights, in order to capture uncertainty in ground motion predictions and avoid bias toward any one model.

The GMPEs were implemented in the model to predict peak ground acceleration (PGA), which was used as the primary intensity measure in this study. However, these GMPEs also support other intensity measures such as spectral acceleration (SA) at different periods. These could be incorporated in future work depending on the needs of engineering design or seismic risk analysis.

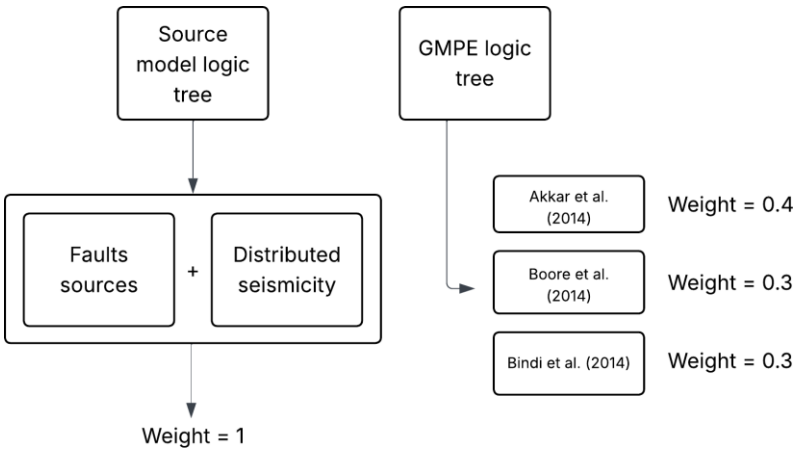

Figure 4: Schematic representation of the logic tree used in the PSHA model.

3.3 Hazard Calculation Parameters

The seismic hazard calculations were carried out using the classical probabilistic method in the OpenQuake Engine. The primary output was peak ground acceleration (PGA), computed at each site for exceedance probabilities of 02%, 05%, and 10% over a 50-year period. These levels correspond to mean return periods commonly used in engineering design and seismic risk assessment.
A rupture mesh spacing of 3 km was applied to discretize fault surfaces, providing a balance between computational efficiency and geometric resolution. For distributed seismicity sources, a minimum magnitude threshold of Mw 4.5 was used, while maximum magnitudes for fault sources were assigned based on fault length (see Table 1)
A maximum source-to-site distance of 300 km was used, meaning that only sources within this radius were considered when calculating ground motion at a given site. This is an appropriate value for tectonic settings characterized by active shallow crust.
Hazard values were computed over a grid of more than 1,500 locations, corresponding to the spatial resolution of the Vs30 dataset. These values enable the development of site-specific seismic hazard maps across the entire study region.

4. Results

The seismic hazard results were computed at 1,540 sites across the Rif area, corresponding to the georeferenced locations in the VS30 site model. Outputs include peak ground acceleration (PGA) hazard maps for selected probabilities of exceedance and hazard curves for key urban centres. These results illustrate the spatial variability of seismic hazard and highlight the influence of both source proximity and local site conditions.

4.1 Hazard Maps

The results of the probabilistic seismic hazard assessment are first presented in the form of peak ground acceleration (PGA) maps for three exceedance probabilities: 10%, 5%, and 02% in 50 years, which correspond to mean return periods of approximately 475, 975, and 2,475 years, respectively. These maps represent the spatial distribution of expected ground shaking across the study area.

The highest hazard values are concentrated in the central and northeastern Rif, particularly around the Al Hoceima, Nekor, and Boudinar fault zones, where both the fault-based and distributed seismicity sources contribute significantly. These areas are characterized by higher expected ground accelerations (up to 0.5g), especially at lower exceedance probabilities.
In contrast, the western Rif and peripheral regions exhibit lower PGA values, reflecting reduced seismicity and the absence of major mapped faults.

As expected, the hazard becomes more pronounced and widespread with decreasing exceedance probability (for longer return periods). The 02% in 50 years map highlights broader zones of high hazard due to the contribution of rarer, larger-magnitude events.

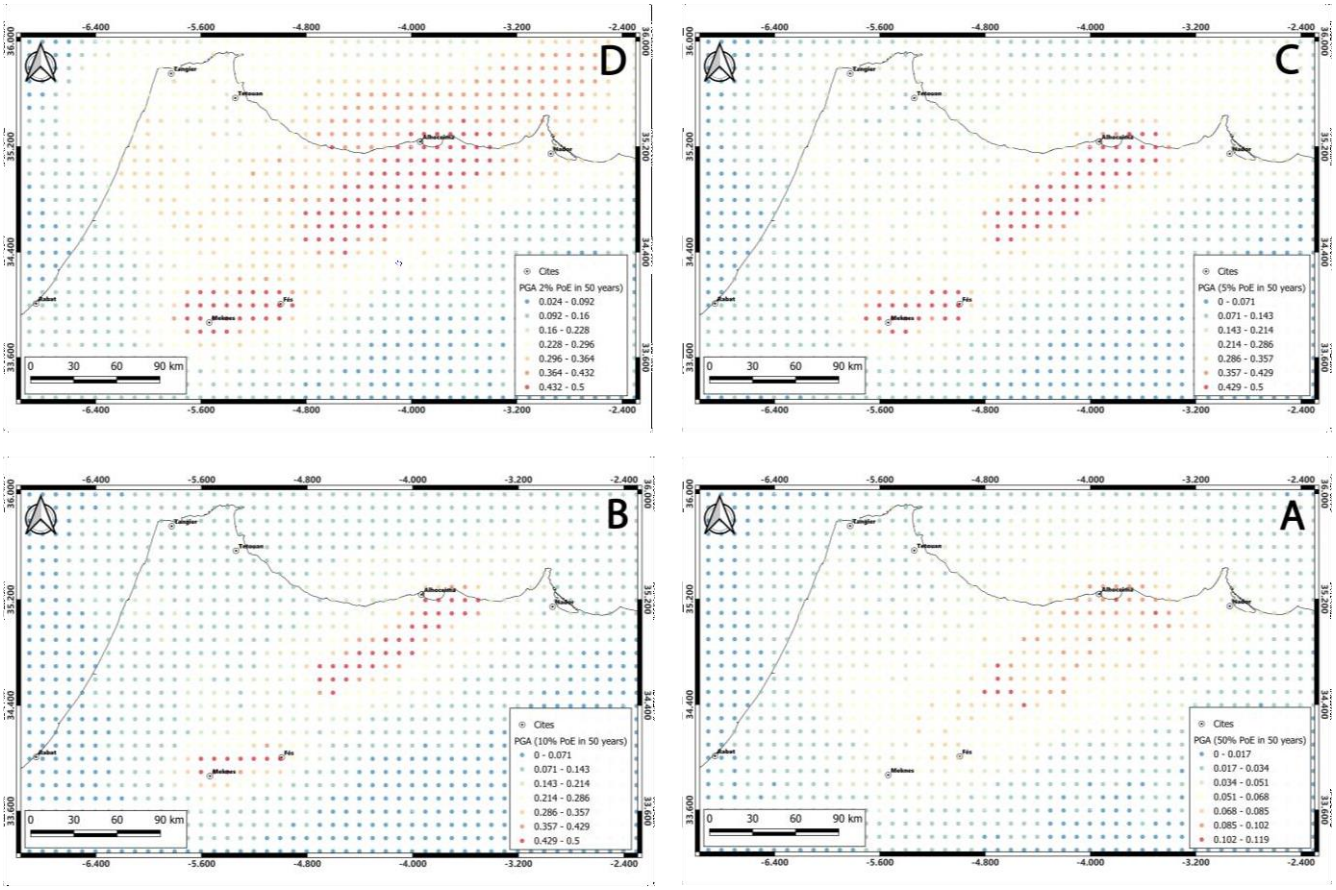

Figure 5 : Seismic hazard maps (PGA) for different probabilities of exceedance in 50 years across the Rif region.
(A) 50% PoE – Return period ~72 years. (B) 10% PoE – Return period ~475 years, (C) 5% PoE – Return period ~975 years, (D) 2% PoE – Return period ~2,475 years

4.2 Hazard Curves

To provide a detailed, site-specific understanding of seismic hazard, representative hazard curves were generated for six major cities in the study area: Al Hoceima, Nador, Tetouan, Fes, Meknes, and Rabat. Each curve represents the average hazard across multiple sites within the city boundaries, calculated by averaging the peak ground acceleration (PGA) values at different probabilities of exceedance (PoE).

These curves illustrate how the likelihood of exceeding various PGA levels decreases with decreasing PoE (increasing return periods). As expected, all curves show a logarithmic decline, with higher probabilities associated with lower PGA thresholds.

Among the six cities, Al Hoceima exhibits the highest seismic hazard across all exceedance levels, reflecting its proximity to active fault systems such as the Al Hoceima and Nekor faults. Nador, Fes and Meknes also show elevated hazard levels, while Rabat, Tetouan and Tangier display relatively lower hazard levels, reflecting their more distal location from high-activity fault zones in the Rif

These findings are visualized in Figure 6, which presents the average hazard curve for each city. The corresponding numerical values are summarized in Table 3, showing the average PGA at multiple PoE levels. These results provide a clear comparison of site-specific hazard across the study area and highlight the importance of regional seismic source characteristics in shaping local ground motion estimates.

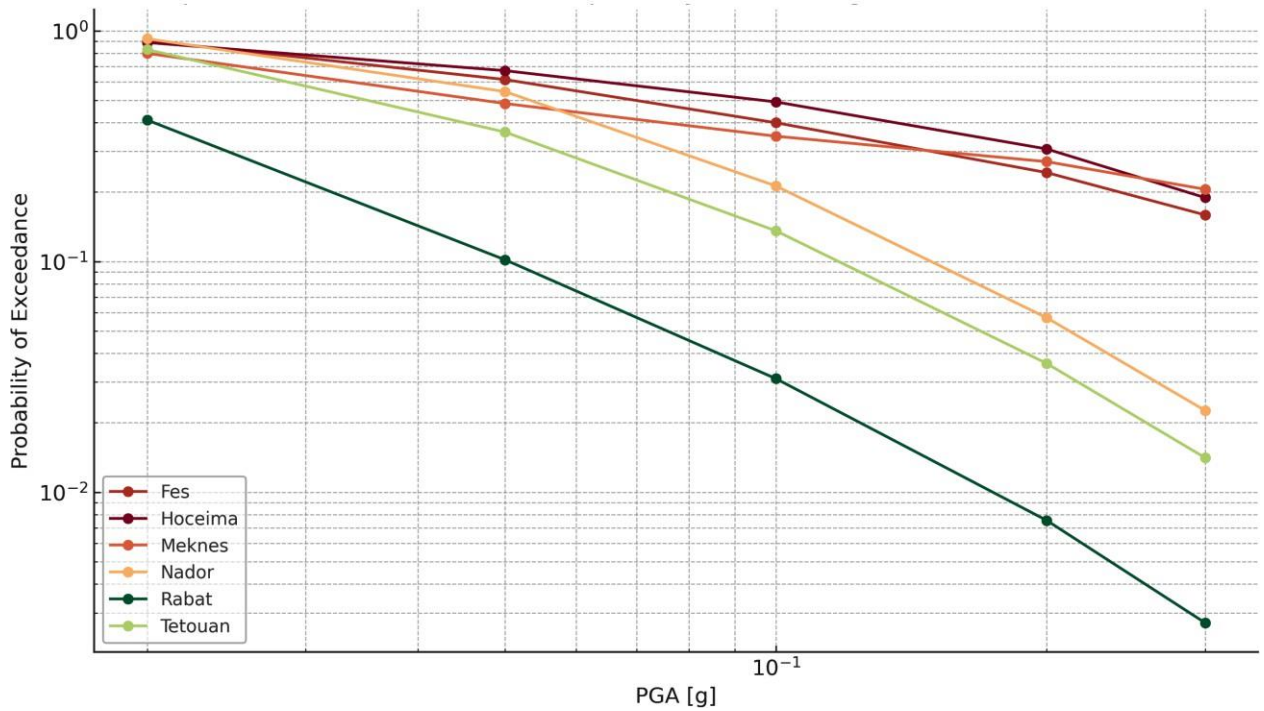

Figure 6: Representative hazard curves for six selected cities, showing average seismic hazard at each city

5. Discussion

The results of the probabilistic seismic hazard analysis (PSHA) conducted in this study reveal spatial patterns and provide insight into seismic hazard across the Rif region. By combining both fault-based sources, modeled using moment-balanced truncated Gutenberg-Richter MFDs, and distributed seismicity zones, represented by incremental MFDs derived from regional earthquake catalogs, the hazard model captures both well-defined fault activity and more diffuse background seismicity. The application of regionally appropriate ground motion prediction equations (GMPEs) further strengthens the physical realism of the model.

The highest hazard levels were observed in the central, (northen and southern Rif), especially in areas near the Nekor, Al Hoceima, and Boudinar fault systems. These zones align with the locations of significant instrumental earthquakes, including the Mw 6.0 Imzouren earthquake (1994), Mw 6.3 Al Hoceima earthquake (2004), and Mw 5.1 Nador earthquake (2016). At a 10% probability of exceedance in 50 years, PGA values range from approximately 0.30 to 0.50 g in these regions.

Notably, inland areas such as Fès and Meknès also exhibit elevated hazard levels, with PGA values ranging from 0.15 to 0.40 g. This is consistent with the presence of active thrust faulting in the southern Rif and Pre-Rif zones,

The hazard curve analysis further emphasizes this pattern. All six cities analyzed, Al Hoceima, Nador, Tetouan, Fès, Meknès, and Rabat, show non-negligible probabilities of exceedance for moderate PGA levels (≥ 0.1 g). In particular, Al Hoceima displays the highest hazard curve, reflecting its proximity to active faults. Fès and Meknès also exhibit substantial hazard, though somewhat lower, due to reverse faulting activity nearby. Fortunately, the recurrence intervals of major events on these faults are long, often exceeding 1,000 years in low-strain areas (Agharroud et al., 2021).

Overall, the combined source model and hazard results provide a detailed understanding of ground motion potential across northern Morocco and highlight the importance of accounting for both mapped fault systems and distributed seismicity when assessing regional hazard.

5.1 Comparison with Moroccan Seismic Design Code (RPS v2011)

The Moroccan Seismic Design Code, RPS v2011, classifies the national territory into five seismic zones based on peak ground acceleration (PGA) values with a 10% probability of exceedance in 50 years. These zones range from Zone Z0 to Zone Z4 as summarized in Table 2; The official seismic zoning map provided in RPS v2011 (see Figure 7) outlines the geographical extent of each zone across the country

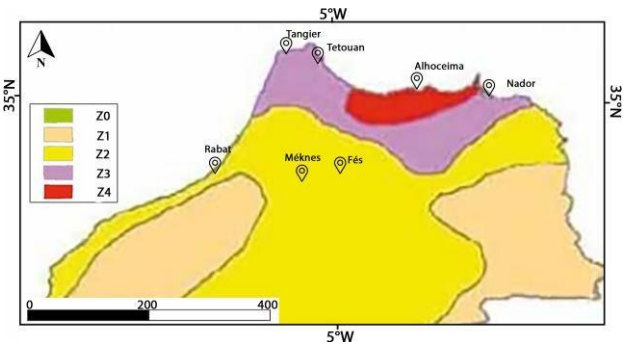

Figure 7: Seismic zoning of northern Morocco as defined in the Moroccan Seismic Design Code (RPS v2011)

Table 2 : Seismic zoning categories and corresponding peak ground acceleration (PGA) values according to the Moroccan Seismic Design Code RPS v2011

Zone	PGA (g)	Seismicity Level
Z0	0.00	Very low seismicity
Z1	0.04	Low seismicity
Z2	0.10	Moderate seismicity
Z3	0.14	High seismicity
Z4	0.18	Very high seismicity

However, the results of this study's probabilistic seismic hazard analysis (PSHA) indicate that the actual ground shaking levels in several major cities may significantly exceed the design thresholds defined in RPS v2011. The mean PGA values computed for a 10% probability of exceedance in 50 years (return period ~475 years) are presented in Table 3 and summarized below:

Table 3: Summary of mean PGA values at 10% probability of exceedance in 50 years for six selected cities.

City	Mean PGA (g)
Al Hoceima	0.49
Fès	0.39
Meknès	0.35
Nador	0.21
Tetouan	0.14
Rabat	0.03

In Al Hoceima, the predicted PGA reaches approximately 0.49 g, nearly three times higher than the value assigned in RPS v2011 for Zone Z4 (0.18 g). Fès and Meknès follow closely, with mean PGA values of 0.39 g and 0.35 g, respectively, both well above the Zone Z2 threshold of 0.14 g. Nador records a value of 0.21 g, placing it above the PGA range used for Zones Z3, while Tetouan at 0.14 g is on the threshold of Zone Z3, which supports its current classification. In contrast, Rabat presents the lowest hazard, with a value of just 0.03 g, consistent with its Zone Z2 assignment.

These results reveal an underestimation of seismic hazard in the current Moroccan seismic design code, particularly in regions affected by active fault systems and recent instrumental seismicity. This study provides a valuable reference and insight into how hazard may be re-evaluated using modern probabilistic methods. The integration of fault-based sources, realistic magnitude-frequency distributions, and regionally appropriate ground motion models produces a hazard model that reflects the tectonic complexity of the Rif and surrounding areas more accurately than the current zonation.

Recent earthquakes, such as the 2023 Al Haouz earthquake, further highlight this gap. Although the region is not classified as high-risk under RPS v2011, the event generated severe ground shaking and caused widespread damage, demonstrating that current zonation may significantly underestimate the seismic potential in some areas. Similar issues are evident in cities like Al Hoceima, Fès, and Meknès, where modeled PGA values in this study greatly exceed the design accelerations set by RPS v2011.

These findings underscore the urgency of updating Morocco's national seismic hazard map and zoning code. While not exhaustive, the present model offers a scientific foundation that could contribute to future revisions. A modernized approach grounded in detailed source modeling, regionally calibrated GMPEs, and site condition data such as Vs30 would ensure that seismic design levels are aligned with the actual hazard levels across Moroccan territory, ultimately improving public safety and structural resilience.

6. Limitations of the Study

While this study presents an improved probabilistic seismic hazard model for the Rif region, several limitations should be acknowledged:

Uncertainty in fault parameters: Many faults in the study area lack well-constrained geometric and kinematic parameters, particularly slip rate and segmentation. Where data are missing or ambiguous, estimates were made based on regional analogs or literature assumptions, which introduces epistemic uncertainty into the model.

Use of global VS30 data: Site amplification effects were modeled using USGS global VS30 estimates based on topographic and geological proxies. These data do not reflect local geophysical measurements and may not accurately capture site-specific soil conditions, especially in urban centers.

Limited spatial resolution of output sites: Hazard computations were performed at 1,540 sites, which provides regional coverage but may not fully resolve localized hazard variations in densely populated areas such as Fès, Al Hoceima, and Meknès. Higher-resolution site modeling and microzonation studies are needed for urban-scale hazard assessment.

Lack of model validation: No formal validation was performed by comparing modeled ground motions with observed accelerometric data from past earthquakes (e.g., 1994, 2004, 2019). Such comparisons would help assess the reliability of the selected GMPEs and the source model structure.

Fixed b-value in magnitude-frequency distributions: The b-value was fixed at 1.0 for all sources based on regional assumptions. While this is common in first-order PSHA models, spatial variability in b-values could influence recurrence estimates and should be explored in future sensitivity studies.

Despite these limitations, the methodology and framework adopted here represent a step forward in seismic hazard modeling in the Rif, and provide a solid basis for further refinement and integration with exposure and vulnerability models in future seismic risk studies.

7. Conclusion

This study presents a probabilistic seismic hazard assessment (PSHA) for the Rif region of northern Morocco using the OpenQuake Engine. The model incorporates both fault-based sources, calibrated through moment-rate balancing, and distributed seismicity zones, characterized by incremental magnitude-frequency distributions derived from earthquake catalogs. Ground shaking was modeled using a logic tree of ground motion prediction equations (GMPEs) selected for their suitability to active shallow crustal environments, which characterize the tectonic setting of the study area.

The results reveal spatial variations in peak ground acceleration (PGA) that exceed the design values outlined in the Moroccan seismic code RPS v2011, especially in cities such as Al Hoceima, Fès, and Meknès. These findings suggest that current zoning may underestimate seismic hazard in several regions, particularly those influenced by active fault systems or recent significant earthquakes.

The model developed in this study aims to highlight the importance and urgency of revising Morocco's seismic zonation. By integrating recent seismic observations, detailed fault-based modeling, and regionally appropriate ground motion prediction equations, this approach provides a more realistic and science-based view of seismic hazard across the country. The results are intended to inform, guide, and support future efforts toward improving national seismic design standards, ensuring they better reflect the actual hazard faced by urban centers in both tectonically active and historically underestimated regions.

Furthermore, recent earthquakes such as the 2023 Al Haouz event, which caused extensive damage in a region previously considered moderate-hazard, reinforce the need for an updated and data-driven seismic zonation. The insights gained from this study may contribute meaningfully to that process by highlighting where current assumptions fall short and how modern PSHA techniques can support more resilient urban planning and infrastructure design across the country.

Acknowledgements

The authors gratefully acknowledge the Hazard Team at the Global Earthquake Model Foundation (GEM) for the training provided on the OpenQuake Engine, which greatly supported the development of this seismic hazard study.

References

Agharroud, K., Siame, L.L., Ben Moussa, A., Bellier, O., Guillou, V., Fleury, J., & El Kharim, Y. (2021). Seismo- Tectonic Model for the Southern Pre- Rif Border (Northern Morocco): Insights from Morphochronology. *Tectonics, 40*, e2020TC006633. https://doi.org/10.1029/2020TC006633

Agharroud, M., et al. (2021). Structural architecture and seismic potential of the central Rif thrust system (Morocco): Constraints from geophysical and geological data. *Tectonophysics, 812*, 228909. https://doi.org/10.1016/j.tecto.2021.228909

Akkar, S., Sandıkkaya, M. A., & Bommer, J. J. (2014). Empirical ground-motion models for point- and extended-source crustal earthquake scenarios in Europe and the Middle East. *Bulletin of Earthquake Engineering, 12*(1), 359–387. https://doi.org/10.1007/s10518-013-9461-4

Asebriy, L., Bourgois, J., Cherkaoui, T.-E., & Azdimousa, A. (1993). Evolution tectonique récente de la zone de faille du Nékor: importance paléogéographique et structurale dans le Rif externe, Maroc. *Journal of African Earth Sciences, 17*(3), 445–457. https://doi.org/10.1016/0899-5362(93)90023-J

Benmakhlouf, M., Galindo-Zaldívar, J., Chalouan, A., Sanz de Galdeano, C., Ahmamou, M., & López-Garrido, A.C. (2012). Inversion of transfer faults: The Jebha–Chrafate fault (Rif, Morocco). *Journal of African Earth Sciences, 73–74*, 33–43. https://doi.org/10.1016/j.jafrearsci.2012.07.003

Bindi, D., Massa, M., Luzi, L., Ameri, G., Pacor, F., Puglia, R., & Augliera, P. (2014). Pan-European ground-motion prediction equations for the vertical component of motion. *Bulletin of Earthquake Engineering, 12*, 1889–1920. https://doi.org/10.1007/s10518-014-9605-z

Boore, D. M., Stewart, J. P., Seyhan, E., & Atkinson, G. M. (2014). NGA-West2 equations for predicting PGA, PGV, and 5% damped PSA for shallow crustal earthquakes. *Earthquake Spectra, 30*(3), 1057–1085. https://doi.org/10.1193/070113EQS184M

Cherkaoui, T.-E., Medina, F., Hatzfeld, D., & Bensaid, M. (1993). Microearthquake seismicity and fault plane solutions around the Nekor strike-slip fault, Morocco. *Earth and Planetary Science Letters, 117*(3-4), 455–469. https://doi.org/10.1016/0012-821X(93)90021-Z

DeMets, C., Gordon, R.G., Argus, D.F., & Stein, S. (1994). Effect of recent revisions to the geomagnetic reversal time-scale on estimates of current plate motions. *Geophysical Research Letters, 21*(20), 2191–2194. https://doi.org/10.1029/94GL02118

Elabbassi, M., Ammar, A., Elouai, D., Harnafi, M., & Hjira, A. (2016). Seismic reflection imaging of active faults and their tectonic behavior in the Northern Moroccan margin: Is the Nekor fault a pure strike-slip fault? *Arabian Journal of Geosciences, 9*, 543. https://doi.org/10.1007/s12517-016-2691-4

Field, E. H., et al. (2009). Uniform California Earthquake Rupture Forecast, Version 2 (UCERF 2). *Bulletin of the Seismological Society of America, 99*(4), 2053–2107. https://doi.org/10.1785/0120080049

Gràcia, E., et al. (2019). Earthquake crisis unveils the growth of an incipient continental fault system. *Nature Communications, 10*, 3482. https://doi.org/10.1038/s41467-019-11064-5

Hanks, T. C., & Kanamori, H. (1979). A moment magnitude scale. *Journal of Geophysical Research, 84*(B5), 2348–2350. https://doi.org/10.1029/JB084iB05p02348

Meghraoui, M., et al. (2016). The Seismotectonic Map of Africa. *Episodes, 39*(1), 9–23. https://doi.org/10.18814/epiiugs/2016/v39i1/89232

Ministry of Housing and Urbanism. (2011). *Moroccan Seismic Design Code RPS 2011 Version*. Rabat, Morocco.

Pagani, M., Monelli, D., Weatherill, G. A., et al. (2014). OpenQuake Engine: An open hazard (and risk) software for the global earthquake model. *Seismological Research Letters, 85*(3), 692–702. https://doi.org/10.1785/0220130087

Peláez, J.A., Henares, J., Hamdache, M., Sanz de Galdeano, C. (2018). A Seismogenic Zone Model for Seismic Hazard Studies in Northwestern Africa. In: D'Amico, S. (eds) Moment Tensor Solutions. Springer Natural Hazards. Springer, Cham. https://doi.org/10.1007/978-3-319-77359-9_29

Poujol, A., et al. (2014). Active tectonics of the Northern Rif (Morocco) from geomorphic and geochronological data. *Journal of Geodynamics, 77*, 70–88. https://doi.org/10.1016/j.jog.2014.01.004

Silva, V., Crowley, H., Pagani, M., Monelli, D., & Pinho, R. (2014). Development of the OpenQuake engine, the Global Earthquake Model's open-source software for seismic hazard and risk assessment. *Natural Hazards, 72*(3), 1409–1427. https://doi.org/10.1007/s11069-013-0618-7

Stich, D., Serpelloni, E., Mancilla, F., & Morales, J. (2006). Kinematics of the Iberia–Maghreb plate boundary from GPS and seismic data. *Tectonophysics, 426*(3–4), 295–317. https://doi.org/10.1016/j.tecto.2006.08.004

Tendero-Salmerón, V., et al. (2021). Application of automated throw backstripping method to characterize recent faulting activity migration in the Al Hoceima Bay (Northeast Morocco): Geodynamic implications. *Frontiers in Earth Science, 9*, 645942. https://doi.org/10.3389/feart.2021.645942

USGS (2023). M6.8 - High Atlas Mountains, Morocco (Al Haouz Earthquake). *United States Geological Survey*. https://earthquake.usgs.gov/

Van der Woerd, J., et al. (2014). The Al Hoceima Mw 6.4 earthquake of 24 February 2004 and its aftershock sequence. *Tectonophysics*. https://doi.org/10.1016/j.jog.2013.12.004

Wells, D. L., & Coppersmith, K. J. (1994). New empirical relationships among magnitude, rupture length, rupture width, rupture area, and surface displacement. *Bulletin of the Seismological Society of America, 84*(4), 974–1002.